# PROBABILISTIC FATIGUE LIFE SENSITIVITY ANALYSIS OF TITANIUM ROTORS

Michael P. Enright and Y.-T. (Justin) Wu
Southwest Research Institute, San Antonio, Texas, 78238

## Abstract

The application of probabilistic methods to the life prediction of fatigue vulnerable structures is becoming increasingly important. In-service inspection and repair/replacement can be an effective strategy for decreasing fatigue failure probability. However, inspection introduces additional random variables that must be considered in an overall lifetime reliability assessment. In this study, a methodology is illustrated to assess the influences of changes in the main descriptors of fatigue related random variables on the lifetime failure probability of an aircraft titanium rotor disk. The methodologies can be used for the development of reliability-based optimal design and maintenance strategies for fatigue vulnerable structures subject to in-service inspection.

## Introduction

The need for the use of non-deterministic methods for fatigue life predictions is becoming increasingly important. Variabilities in fatigue strength data and in the relationship between stress range and fatigue life for a given material can be significant[1,2]. A probabilistic fatigue evaluation can take into account these and other uncertainties associated with fatigue failure of structures and mechanical components.

Design-Assessment-of-Reliability-With-Inspection (DARWIN*) is a computer program that integrates finite element stress analysis, fracture mechanics analysis, non-destructive inspection simulation, and probabilistic analysis to assess the risk of rotor fracture with in-service inspection. DARWIN computes the probability-of-fracture versus flight cycles considering random defect occurrence and location, random inspection schedules, multiple inspections, and other random variables[3].

In this study, the influences of changes in the main descriptors of fatigue related random variables on the lifetime failure probability of an aircraft titanium rotor disk is illustrated using the DARWIN computer program. It is shown that, compared to the other random variables considered, the defect size can have a dominant influence on the lifetime reliability of turbine rotor disks. In addition, for the rotor disk considered, inspection time variability does not appear to have a significant effect on lifetime reliability, but does influence the optimum mean inspection time. The results can be used for the development of reliability-based optimal design and maintenance strategies for fatigue vulnerable structures subject to in-service inspection.

## Fatigue Reliability Prediction Using DARWIN

The fatigue failure probability is defined as the probability of violating the fatigue limit state $g(\boldsymbol{X}, \boldsymbol{Y}, t)$. Fatigue failure occurs when the stress intensity factor $K$ exceeds the fracture toughness $K_C$ :

$$g(\boldsymbol{X},\ \boldsymbol{Y},\ t)\ =\ K_C - K(\boldsymbol{X},\ \boldsymbol{Y}, t)\ \leq\ 0 \qquad (1)$$

where $\boldsymbol{X}$ is a vector of input variables unrelated to inspections, $\boldsymbol{Y}$ is a vector of input variables related to inspections, and $t$ is flight hours[4]. A negative or zero value of $g(\boldsymbol{X}, \boldsymbol{Y}, t)$ represents a failure event.

Vector $\boldsymbol{X}$ consists of three key random variables: initial defect area, stress, and life. The initial defect area is represented using a defect distribution based on historic data developed by the Rotor Integrity Sub Committee (RISC) of the Aerospace Industries Association[5]. The stress random variable is modeled as the product of deterministic stress and a random variable $X_1$ as follows:

$$\sigma = X_1 \cdot \sigma_{FEM} \qquad (2)$$

where $X_1$ is the stress multiplier, a random variable accounting for the errors in geometry and numerical

*DARWIN™ is a registered trademark of Southwest Research Institute.

"Copyright © 2000 by Southwest Research Institute. Published by the American Institute of Aeronautics and Astronautics, Inc. with permission."

(e.g., finite element) modeling, and $\sigma_{FEM}$ is the deterministic stress obtained from finite element analysis (adjusted to account for residual stresses). The life $N$ is also modeled as the product of a deterministic variable and a random variable:

$$N = X_2 \cdot N_{\text{model}} \tag{3}$$

where $N_{model}$ is the deterministic life computed using fracture mechanics methods, and $X_2$ is the life scatter random variable accounting for the modeling error in the deterministic life model and the variability due to stochastic crack growth.

Vector $Y$ contains the inspection related random variables, and consists of the POD (probability of detection) curve and the inspection time. The POD curves are represented using default distributions provided by RISC[5]. The inspection time is modeled as a normally distributed random variable. Eqns. (1)-(3) provide a focus on the key random variables influencing fatigue failure of rotor disks. A detailed description of the probabilistic methodology implemented in DARWIN is presented elsewhere [3,6].

## Parametric Sensitivity Analysis

Consider the titanium ring disk model shown in Fig. 1. Assume that the design life of the disk is 20,000 flight cycles, and the maximum disk speed during each flight cycle is 6,000 RPM. A 50 MPa external pressure load is applied to the outer surface of the disk to simulate blade loading. A single inspection is performed at about 10,000 cycles, and all disks with detected defects are removed. The initial defect area and POD are based on default distributions provided by RISC[5]. This disk model is based on the parameters found in an associated FAA Advisory Circular (AC) and is referred to as the AC Test or AC Base Case. Additional details regarding this model and associated data are presented elsewhere[7].

DARWIN uses a zone based risk computation procedure, in which a component is partitioned into zones of approximately equal risk. The material properties, stresses, and temperatures within each zone are approximately constant. The disk is divided into 21 zones (Fig. 2). Subsurface defects are located in the geometric center of the interior zones, and surface defects are located on the exterior surfaces of the exterior zones. For design applications, it may be preferable to place defects at the minimum-life locations to achieve conservative solutions.

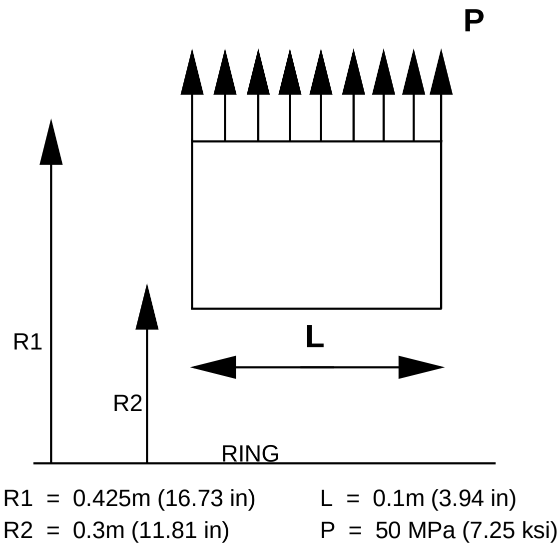


**Figure 1: Rotor Disk Example - Geometry and Loading**

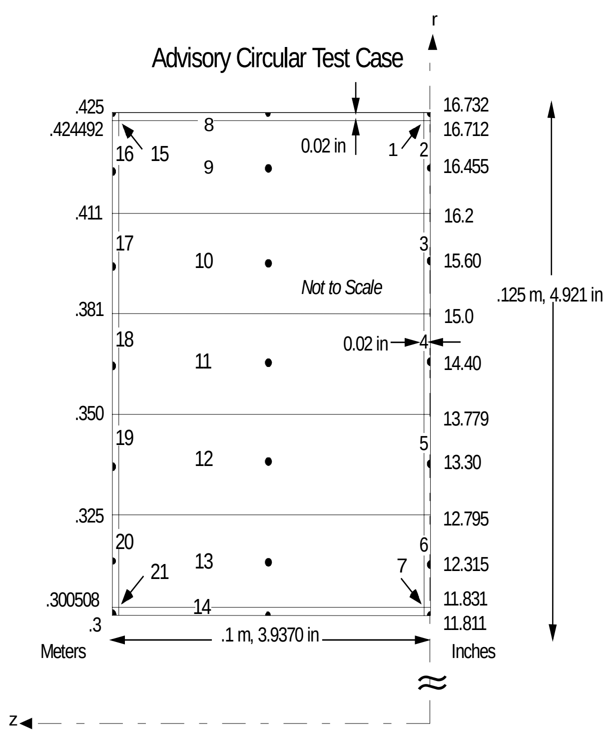


**Figure 2: Zone Definition and Initial Defect Locations**

**Table 1: Definition of Random Variables for Sensitivity Analysis**

| VARIABLE | NOMINAL VALUE | RANGE |
|---|---|---|
| Stress Multiplier Median | 1.0 | 0.7 - 1.3 |
| Stress Multiplier COV | 0.0 | 0% - 30% |
| Life Scatter COV | 0.0 | 0% - 30% |
| Inspection Time Mean (Cycles) | 10,000 | 1,000 - 20,000 |
| Inspection Time COV | 0.0 | 0% - 30% |
| Maximum Defect Area ($mil^2$) | Defined by Defect Exceedance Curve | 1,000 - 200,000 |

It is assumed that the probability of occurrence of a single defect in each zone is very small, and the probability of occurrence of two defects within the same zone is negligible (consistent with the observed defect occurrence rate in titanium disks).

Values for the input random variables are indicated in Table 1. The following variables were considered in the sensitivity analysis: stress multiplier median and COV, life scatter COV, inspection time mean value and COV, and the maximum area in the defect exceedance curve. The stress factor and life scatter are both lognormally distributed with a default median of 1.0, and the inspection time is normally distributed.

An exceedance curve for a quantity of material, W, (e.g., W = one million pounds) is used to characterize the defect occurrence rate and defect area distribution (Fig. 3). A defect cumulative distribution function, CDF, is defined as follows:

$$CDF = 1 - \frac{N_d(a) - N_d(a_{\max})}{N_d(a_{min}) - N_d(a_{max})} \quad (4)$$

where $N_d(a)$ is the expected number of defects of area $a$ in W, and $a_{min}$ and $a_{max}$ are the minimum and maximum defect areas, respectively. The absolute upper bound of the defect area corresponds to $N_d(a) = 0$.

The probability $P_{detected}$ of detecting a defect from a population of defects is :

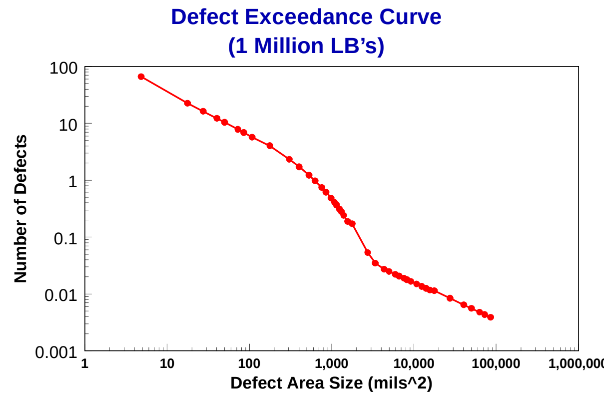

Figure 3: Defect Exceedance Curve for Titanium Rotor Disk Materials[5]

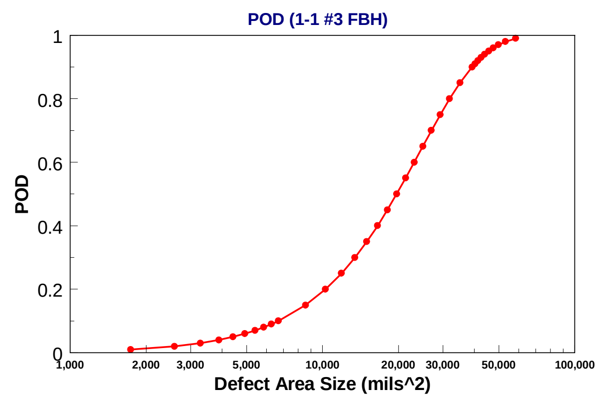

Figure 4: POD (Probability of Detection) Curve[5]

$$P_{detected} = \int_0^{\infty} POD(a) \cdot f(a)\, da \quad (5)$$

where *POD(a)* is the probability of detecting a defect with a size (area) greater than *a* and *f(a)* is the probability density function associated with *a*. The POD used in this example is shown in Fig. 4.

COV values were varied from 0% to 30% in 5% increments. The stress multiplier median was varied from 0.7 to 1.3 in 0.1 increments. Mean inspection times were varied from 1,000 cycles to 20,000 cycles in 1,000 cycle increments. The maximum defect area (defect exceedance curve) was set at values ranging from 1,000 $mil^2$ to 200,000 $mil^2$ (i.e., 1,000; 2,000; 5,000; 10,000; 20,000; 50,000; 100,000; and 200,000 $mil^2$). The defect exceedance values associated with the selected maximum defect areas were computed using linear interpolation or extrapolation on a log-log (base

10) scale. Risk computations[6] were performed using both Monte Carlo simulation (10,000 and 100,000 samples) and importance sampling (100 and 400 samples).

## Results

As shown in Fig. 5, the stress multiplier COV has a significant influence on the probability of fracture at 20,000 cycles (i.e., lifetime failure probability $P_f$ ), and increases nonlinearly with increasing stress COV. The $P_f$ associated with 30% stress COV is more than an order of magnitude higher than the $P_f$ associated with 0% stress COV for both the inspection and no inspection cases. The change in lifetime failure probability due to inspection appears to increase slightly as the stress COV is increased, however, this change is relatively minor compared with the overall increase in $P_f$. In Fig. 6, the influence of the stress multiplier median on $P_f$ is shown. Similar to the stress multiplier COV, the influence of the stress multiplier median on $P_f$ is significant. $P_f$ increases three to four orders of magnitude for stress multiplier median range 0.7 to 1.3. The results of Figs. 5 and 6 suggest that reducing the stress or stress variation, if possible, is an effective way of reducing $P_f$, perhaps more effective than implementing inspection.

The influence of the life scatter COV on the probability of fracture at 20,000 cycles is shown in Fig. 7. As the life scatter COV is increased from 0% to 30%, $P_f$ increases 60% to 80% for the inspection and no inspection cases. The $P_f$ reduction due to inspection is approximately constant for the range of COV studied.

In Fig. 8, the effect of varying the mean inspection time is shown for deterministic inspection (i.e., inspection time COV = 0). $P_f$ reaches the minimum when the inspection is performed at approximately 14,000 cycles. The inspection time COV has an influence on the value of the optimum mean inspection time that minimizes the probability of fracture at 20,000 cycles. In Fig. 9, it can be observed that the optimum mean inspection time varies from 12,000 cycles to 14,000 cycles for inspection time COVs ranging from 0% to 30%.

The expected value of $P_f$ can be defined in terms of the inspection time probability density function *f(t)*:

$$P_f = \int P_f^C(t)\, f(t)\, dt \qquad (6)$$

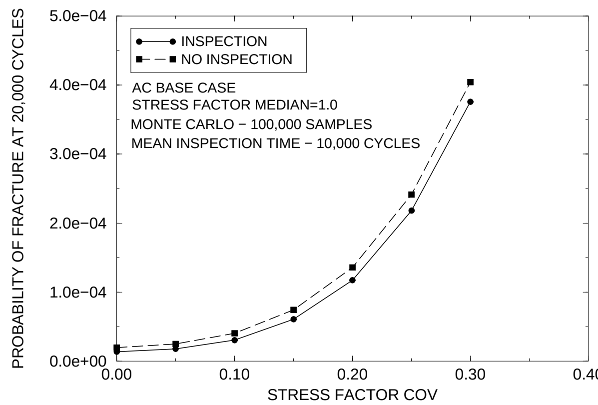


**Figure 5: Influence of Stress Multiplier Factor COV on Lifetime Failure Probability**

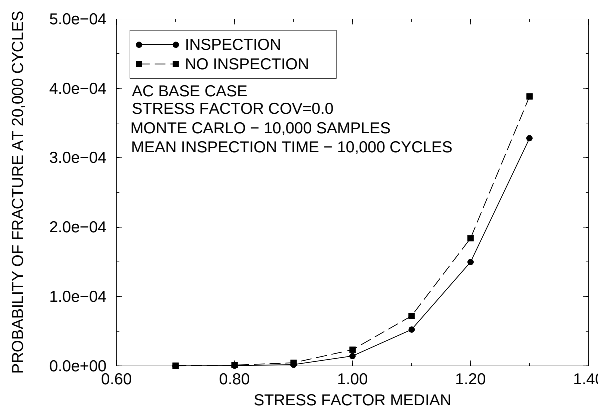


**Figure 6: Influence of Stress Multiplier Factor Median on Lifetime Failure Probability**

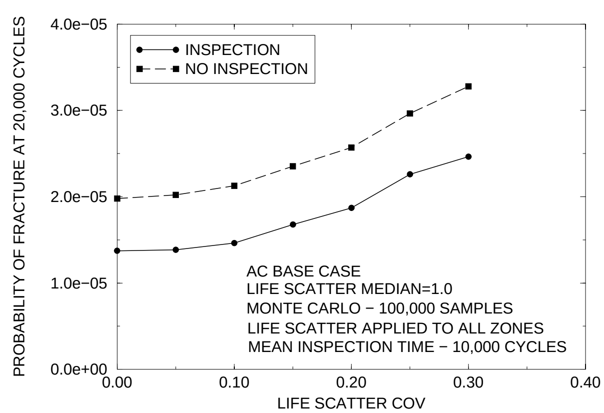


**Figure 7: Influence of Life Scatter COV on Lifetime Failure Probability**

where $P_f^C(t)$ is the probability of failure given inspection time $t$. Suppose an inspection time $t_{opt}$ exists that minimizes $P_f^C(t)$:

$$P_f^C(t_{opt}) \le P_f^C(t) \tag{7}$$

then

$$\int P_f^C(t_{opt})\, f(t_{opt})\, dt_{opt} = P_f^C(t_{opt}) \tag{8}$$

and

$$P_f^C(t_{opt}) \le \int P_f^C(t)\, f(t)\, dt \tag{9}$$

Furthermore, if *f(t)* is symmetric about $t_{opt}$ (i.e., skew=0), then $P_f$ decreases with decreasing inspection time COV.

In Fig. 10, the influence of inspection time COV on probability of fracture at 20,000 cycles is shown for a mean inspection time of 10,000 cycles. Also shown are failure probabilities for the optimum mean inspection times associated with minimum probability of fracture at 20,000 cycles. It can be observed that $P_f$ is relatively insensitive to inspection time COV if the inspection is performed at 10,000 cycles. If the optimum mean inspection time is used, however, $P_f$ may be significantly lower than that for 10,000 cycles and increases with increasing COV values. The result suggests that the optimal mean inspection time is dependent on inspection time COV.

For inspection time COV = 0, the $P_f$ obtained at the optimal mean inspection time represents a lower bound (i.e., minimum $P_f$ for all values of inspection time COV). This lower bound value illustrates the maximum influence of inspection on failure probability reduction.

A comparison of the influences of stress, life scatter, and inspection time COVs on $P_f$ is shown in Fig. 11. It can be observed that stress COV has a dominant effect on $P_f$. In fact, the $P_f$ associated with 10% stress COV is larger than the failure probabilities associated with 30% COV for life scatter and inspection time. This illustrates that a reduction in the stress COV can have more influence on reducing $P_f$ as compared to the life scatter and inspection time COVs.

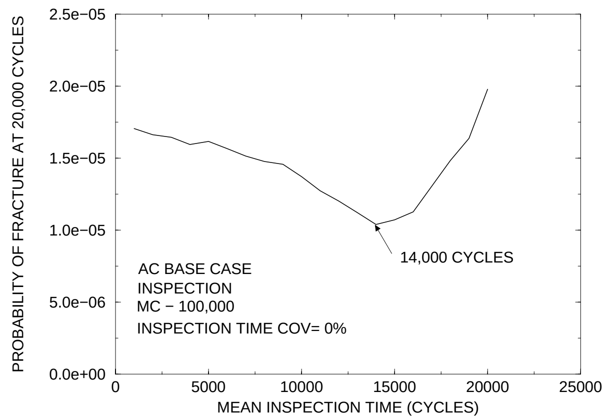


**Figure 8: Optimum Mean Inspection Time for Minimum Lifetime Failure Probability**

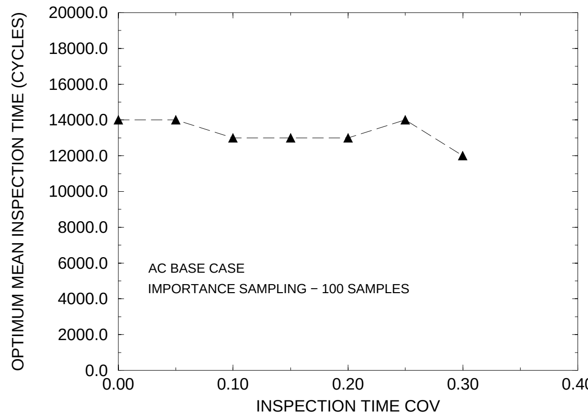


**Figure 9: Influence of Inspection Time COV on Optimum Mean Inspection Time**

In Fig. 12, the influence of the maximum defect area is shown for maximum defect areas ranging from 1,000 to 200,000 mil$^2$. It can be observed that the most significant increases in $P_f$ occur in the range of 1,000 - 5,000 mil$^2$. In this region, $P_f$ increases roughly up to six (or more) times its value for both the inspection and no inspection cases. Reduction in $P_f$ due to inspection increases with increasing maximum defect area.

## Importance Sampling Based Risk Sensitivity Analysis Capability Development

The sensitivity of the lifetime failure probability $P_f$ with respect to changes in the standard deviation $\sigma_i$ of a random variable $i$ can be evaluated from[4]:

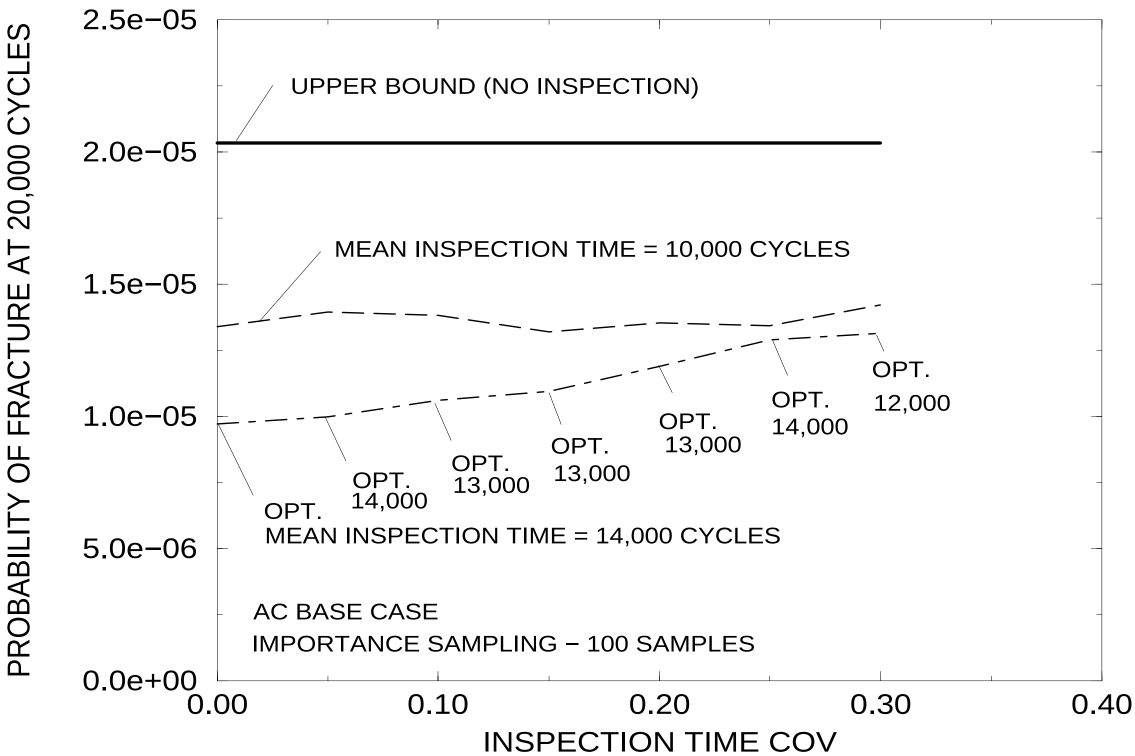


**Figure 10: Influence of Inspection Time COV on Lifetime Failure Probability**

$$S_{\sigma_i} = \frac{\partial P_f / P_f}{\partial \sigma_i / \sigma_i} = \int_\Omega \cdots \int \frac{\sigma_i}{P_f} \frac{\partial f_x}{f_x \partial \sigma_i} f_x \, dx \qquad (10)$$

where $S_{\sigma_i}$ is the sigma (standard deviation) sensitivity coefficient, $f_x$ is the joint probability density function of the random variables associated with $P_f$, and $\Omega$ is the sampling domain.

If all variables are independent and normally distributed, the sigma sensitivity coefficient becomes[8]

$$S_{\sigma_i} = E\left[\left(\frac{X_i - \mu_i}{\sigma_i}\right)^2 - 1\right]_\Omega \qquad (11)$$

where $X_i$ is a continuous random variable, and $\mu_i$ is the mean of random variable *i*.

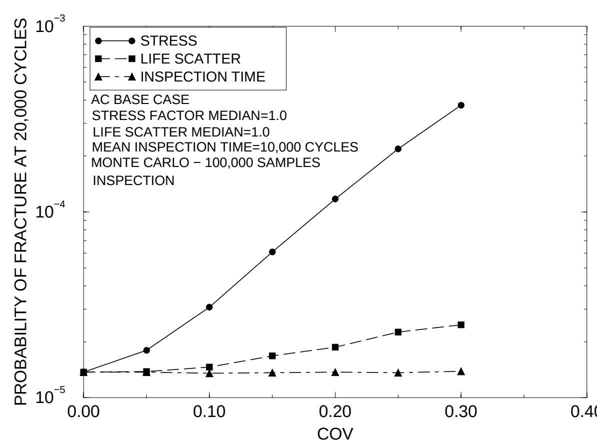


**Figure 11: Comparison of the Influences of Stress, Life Scatter, and Inspection Time COVs on Lifetime Failure Probability**

An importance sampling-based risk sensitivity analysis capability is currently under development for the DARWIN computer program. The approach is illustrated for a critical zone with highest (conditional) $P_f$ (Zone 13, Fig. 2). DARWIN is used to generate 100 samples that fall within the failure region (i.e., life < 20,000 cycles) if no inspection is performed. Stress scatter and defect sizes associated with the generated samples are shown in Fig. 13.

Using the samples shown in Fig. 13, the sensitivity of the probability of failure, $P_f$ , with respect to the changes in the standard deviations of the stress scatter, life scatter, and defect size were computed using the Matlab computer program. A median value of 1.0 was used for stress scatter and life scatter. A COV value of 10% was used for stress scatter, and a range of COV values (10%, 30%, 50%) were used for life scatter. The main descriptors of the defect distribution were approximated based on a curve fit of a default defect exceedance curve (Fig. 3). The distribution was assumed to be lognormal, and the curve fit was focused on the right tail (i.e., larger defect size).

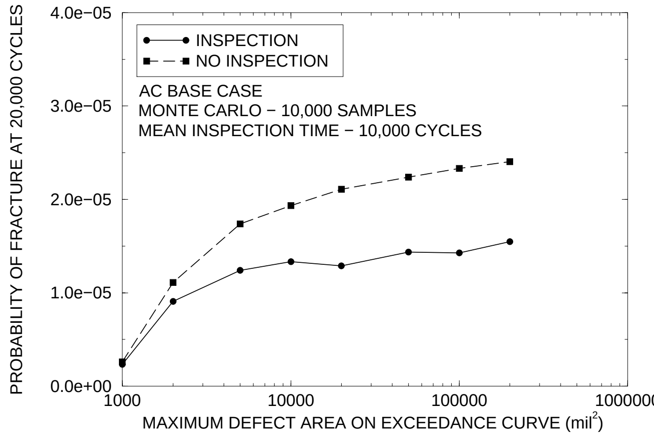


**Figure 12: Influence of Maximum Defect Area on Lifetime Failure Probability**

The preliminary result, shown in Fig. 14, suggests that the defect size is the most dominant random variable, as expected. The result also suggests that the life scatter has a minimal contribution, assuming a COV of 10 % for both the life scatter and the stress scatter multiplier.

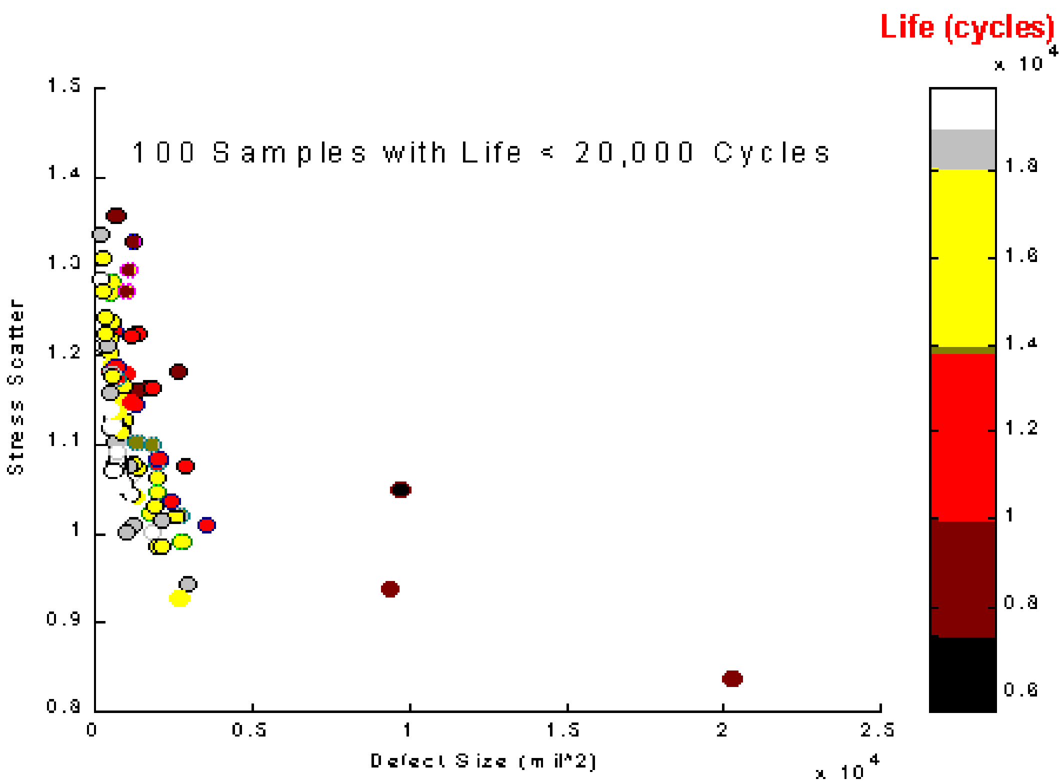


**Figure 13: Samples Generated from DARWIN for Risk Sensitivity**

Fig. 15 shows that when the life scatter COV is increased from 10% to 50%, the life scatter sensitivity increases from 1.5% to 20% of the defect-size sensitivity. Although this result is preliminary, it strongly suggests that this type of risk sensitivity information, which can be obtained very efficiently (i.e., as a by-product of DARWIN analysis), is useful for determining whether more accurate data or probabilistic models are needed for stress and life variables.

## Conclusions

The lifetime reliability of fatigue vulnerable structures is dependent on a number of random variables, especially if the influences of in-service inspection are considered. In this study, the DARWIN computer program was used to illustrate the relative influences of several fatigue-related random variables on the lifetime failure probability of an aircraft engine rotor disk. For the range of fatigue random values considered in this study, the following general conclusions can be made:

1. Relative to life scatter and stress scatter, the defect size has a dominant effect on lifetime failure probability. The extent of this influence is dependent on the relative COV magnitudes among these three key random variables.

2. Compared to life scatter and inspection time variability, the stress median or COV has the most influence on lifetime failure probability. Reducing the stress or stress variation, if possible, is an effective way of reducing $P_f$, perhaps even more

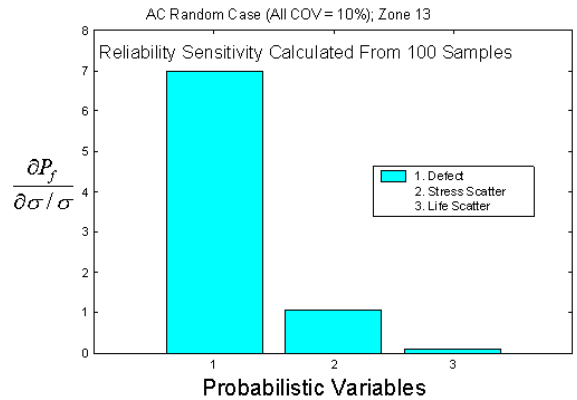


**Figure 14: Importance Sampling-Based Risk Sensitivity Analysis Can Be Used to Identify and Rank Influential Probabilistic Variables (Currently Under Development)**

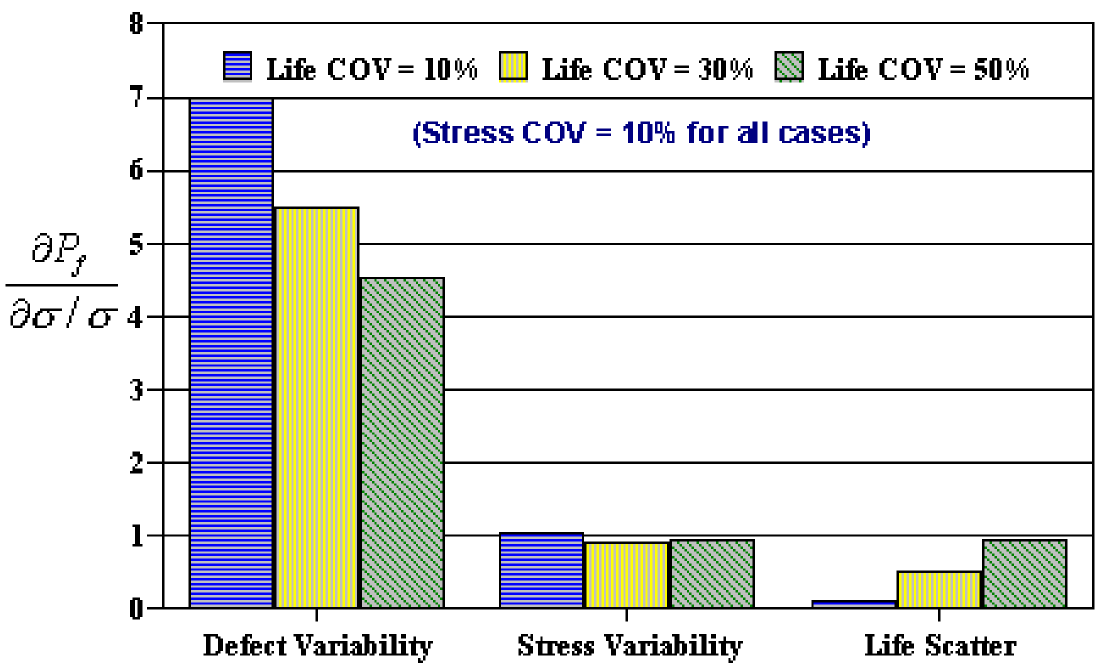


**Figure 15: Influence of Life Scatter COV on Risk Sensitivity Analysis**

effective than implementing inspection.

3. As expected, the mean inspection time can have a large influence on lifetime failure probability. However, inspection time variability (i.e., COV) does not appear to have a significant impact on $P_f$, particularly if the mean inspection time is not at the optimal time.

4. Optimal mean inspection time depends on the inspection time COV. *Pf* approaches a lower bound value as inspection time COV approaches 0, which illustrates the maximum influence of inspection on failure probability reduction.

The most critical defect sizes are in the range of 1,000 - 5,000 mil$^2$. Very large defects (> 5,000 mil$^2$) do not significantly increase $P_f$ because the probability of occurrence is relatively small in the default distribution.

These conclusions are based on an idealized rotor disk for a specific geometry, load condition, defect distribution, and POD. Results obtained for in-service turbine rotor disks under different assumptions may differ from the results presented in this study.

## Acknowledgements

This work was performed as part of the Titanium Rotor Materials Design (TRMD) project supported by the Federal Aviation Administration under Cooperative Agreement 95-G-041. Mr. Bruce Fenton, Mr. Joe Wilson, and Mr. Timoleon Mouzakis of the FAA are thanked for their guidance and support. The extensive contributions and cooperation of the many industry members of the program team and its Steering Committee have been essential to program success and are deeply appreciated.

## References

1. Byers, W.G., Marley, M.J., Mohammadi, J., Nielson, R.J., Sarkani, S. (1997). "Fatigue reliability reassessment procedures: state-of-the-art paper," *Journal of Structural Engineering*, **123** (3), 271-276.

2. Tobias, D.H., and Foutch, D.A. (1997). "Reliability-based method for fatigue evaluation of railway bridges," *Journal of Bridge Engineering*, ASCE, **2** (2), 53-60.

3. Millwater, H.R., Fitch, S., Riha, D.S., Enright, M.P., Leverant, G.R., McClung, R.C., Kuhlman, C.J., Chell, G.G., Lee, Y.-D. (2000). "A probabilistically-based damage tolerance analysis computer program for hard alpha anomalies in titanium rotors," *Proceedings, 45th ASME International Gas Turbine & Aeroengine Technical Congress*, Munich, Germany, May 8-11.

4. Wu, Y-T. (1994). "Computational methods for efficient structural reliability and reliability sensitivity analysis," *AIAA Journal*, **32** (8), 1717-1723.

5. Aerospace Industries Association Rotor Integrity Subcommittee (1997). "The development of anomaly distributions for aircraft engine titanium disk alloys," *Proceedings, 38th Structures, Structural Dynamics, and Materials Conference*, Kissimmee, FL, April 7-10, 2543-2553.

6. Wu, Y-T., Enright, M.P., McClung, R.C., Millwater, H., Leverant, G.R. (2000). "Probabilistic methods for design assessment of reliability with inspection (DARWIN)," *Proceedings, 41st Structures, Structural Dynamics, and Materials Conference*, Atlanta, GA, April 3-6.

7. Southwest Research Institute, Allied Signal, General Electric, Pratt and Whitney, Rolls-Royce Allison, Scientific Forming Technologies (1999). *Turbine Rotor Material Design*, Final Report, FAA Grant 95-G-041, Federal Aviation Administration, Washington, D.C.

8. Wu, Y-T. (1999). "An efficient method for reliability analysis of structures subjected to in-service inspections," *Proceedings, 13th ASCE Engineering Mechanics Division Conference*, Baltimore, MD, June 13-16.